

A Phenomenological Theory of Superconductor Diodes in Presence of Magnetochiral Anisotropy

James Jun He¹, Yukio Tanaka², Naoto Nagaosa^{1,3}

¹ *RIKEN Center for Emergent Matter Science (CEMS), Wako, Saitama 351-0198, Japan*

² *Department of Applied Physics, Nagoya University, Nagoya 464-8603, Japan*

³ *Department of Applied Physics, The University of Tokyo, Tokyo 113-8656, Japan*

(Dated: June 8, 2021)

Nonreciprocal responses in noncentrosymmetric systems contain a broad range of phenomena. Especially, non-dissipative and coherent nonreciprocal transport in solids is an important fundamental issue. The recent discovery of superconductor diodes under external magnetic fields, where the critical current changes as the direction is reversed, significantly boosted this research area. However, a theoretical understanding of such phenomena is lacking. Here, we provide theoretical descriptions of superconductor and Josephson junction diodes with the Ginzburg-Landau method. The theory is applied to a few typical systems, where the analytical relations between the nonreciprocal critical currents and the system parameters are obtained. Long Josephson junctions near the superconducting transition temperature under weak fields are studied analytically, while broader parameter regimes are investigated numerically. These results offer a unified description and design principle of superconductor diodes.

INTRODUCTION

Nonreciprocity in materials [1] means that physical quantities changes when the observation direction is reversed. This phenomena has been well studied in semiconductors and it plays a key role in modern technologies such as electrical diodes and solar cells. A new developing subject related to this topic is the contribution by the Berry phase of the electronic states [2], such as shift currents [3].

In recent years, nonreciprocity in superconductors (SCs) has emerged as an rather active research topic [4–7]. When both inversion and time-reversal symmetries are broken, magnetochiral anisotropy [1, 8] is induced and the conductance near the superconducting transition temperature $T \approx T_c$, i.e. the paraconductivity, becomes different if the current direction is inverted. The difference is greatly enhanced as the superconducting order parameter Δ_{sc} develops. This enhancement may be understood as a result of replacing E_{so}/E_F (E_{so} being the spin-orbit splitting and E_F the Fermi energy) by E_{so}/Δ_{sc} [5], which qualitatively determine the strengths of the nonreciprocities in normal and superconducting systems respectively.

The research on nonreciprocity in SCs has been further promoted by the recent discovery of the superconductor diode effect [9], where the critical current depends on the current-flowing direction, i.e. $I_{c+} \neq I_{c-}$. As a result, a superconductor diode has zero resistance along one direction but nonzero along the other. This discovery is followed by the observation of its Josephson-junction version [10], which allows even stronger nonreciprocity due to the reduced Δ_{sc} in the junction region. These works make great steps towards coherent superconducting de-

vices. However, a theoretical description of the superconductor diode effect is absent. Such a theory is needed not only for understanding but also for further experimental development. In the case of Josephson junctions, the diode effect was once proposed in a time-reversal invariant system [11]. This theory relies on strong electron-electron interaction and require the SCs on the two sides of the junction to be in different parameter regions. This does not apply to the recently observed Josephson diode effect [10], which clearly relies on the external magnetic field and should originate from spin-orbit coupling. A previous calculation in a relevant system with Ginzburg-Landau (GL) theory obtained anomalous behaviour in the current phase relation (CPR), but I_{c+} and I_{c-} there are equal [12]. On the other hand, differences between I_{c+} and I_{c-} were seen in specific model systems [13–20]. However, they were largely regarded as a bonus of the anomalous CPR, and a general understanding is lacking.

Here, we provide a phenomenological theory of superconductor diodes with the GL method. We show that the third order term in the Cooper pair spatial variation, $\partial_r^3 \Delta_{sc}(\mathbf{r})$, plays a crucial role in SC diode effects, while previous research with such terms only discussed the paraconductivity [4, 5]. We apply our theory to various spin-orbit coupled systems including (a) Rashba SCs, (b) superconducting surface states of topological insulators, and (c) Ising SCs. We obtain the analytical relations between the strengths of the SC diode effects and the corresponding system parameters. We further generalize the theory to Josephson junctions, where the symmetry requirement to obtain nonreciprocal Josephson current is discussed and numerical results based on lattice models are provided.

RESULTS

In presence of spin-orbit coupling (SOC) and a magnetic field, the GL free energy of a superconductor can be written as

$$F = \int d\mathbf{q} \{ (\alpha + \gamma q^2 + \gamma' q^4 + \eta_{\mathbf{q}}) |\psi_{\mathbf{q}}|^2 + \frac{\beta}{2} |\psi_{\mathbf{q}}|^4 \}. \quad (1)$$

where $\psi_{\mathbf{q}}$ is the order parameter in the reciprocal space, and

$$\eta_{\mathbf{q}} = h \sum_{lmn} \kappa_{lmn} q_x^l q_y^n q_z^m \quad (2)$$

is induced by breaking inversion (\mathcal{P}) and time-reversal (\mathcal{T}) symmetries ($l+m+n$ being an odd integer), responsible for the magnetochiral anisotropy. The magnetic field h is assumed small. The parameters $\alpha \sim T - T_c$, $\beta > 0$ and $\gamma > 0$ are conventional GL coefficients. A positive γ' is introduced to guarantee the stability of the ground state.

Symmetry analysis

The structure of the coupling constants κ_{lmn} is directly related to the symmetries of the system and thus to the form of SOC. For example, in a system with continuous rotational symmetry \mathcal{C}_{∞} (rotation axis along \hat{z}), the group representation determines that $\eta_{\mathbf{q}} = (a_0 + a_2 |\mathbf{q}|^2) (\mathbf{h} \cdot \mathbf{q}) + (b_0 + b_2 |\mathbf{q}|^2) (\mathbf{h} \times \mathbf{q}) \cdot \hat{z}$, up to the linear order in h and the third order in \mathbf{q} . The $\mathbf{h} \cdot \mathbf{q}$ term breaks all mirror symmetries, while $(\mathbf{h} \times \mathbf{q}) \cdot \hat{z}$ breaks the mirror symmetry in the z -direction, \mathcal{M}_z . When \mathcal{C}_{∞} is reduced to discrete rotation \mathcal{C}_n , a form of $\eta_{\mathbf{q}} = (c_1 |\mathbf{q}_{\parallel}| + c_3 |\mathbf{q}_{\parallel}|^3) h_z \cos(n\theta_{\mathbf{q}_{\parallel}})$ is allowed, which respects \mathcal{M}_z . Examples of the above situations will be encountered in this manuscript.

In general, even if both \mathcal{P} and \mathcal{T} are broken, nonreciprocal effects are not necessarily expected. To see that, let us define the inversion operators of each dimension, $\mathcal{P}_x, \mathcal{P}_y$ and \mathcal{P}_z by requiring that $\mathcal{P}_{x/y/z} H(k_{x/y/z}) \mathcal{P}_{x/y/z}^{-1} = H(-k_{x/y/z})$ respectively, where $H(\mathbf{k})$ is the Hamiltonian of the system. Obviously $\mathcal{P} = \mathcal{P}_x \mathcal{P}_y \mathcal{P}_z$ is broken as long as $l+m+n$ is odd in Eq. (2). However, since breaking \mathcal{P}_x (also referred to as chiral symmetry [34]) is necessary for any possible difference between the currents along the $\pm x$ directions, a term such as $h q_x^2 q_y$, although breaking \mathcal{P} and \mathcal{T} , would not cause such a nonreciprocity. This means that the magnetic field to induce nonreciprocal effects needs to be determined by symmetries — it should break all possible \mathcal{P}_x of the Hamiltonian. This will be illustrated with the examples discussed in the later part of this paper.

Superconductor diodes

Let us consider the case where the magnitude of the

SC order parameter is uniform and it only varies in its phase along the x -direction, i.e. $\psi(\mathbf{r}) = |\psi| e^{i\phi(x)}$. In this simplified case, the free energy becomes

$$F = \int dq \{ [\alpha + \gamma q^2 + \gamma' q^4 + hq(\kappa_1 + \kappa_3 q^2)] |\psi|^2 + \frac{\beta}{2} |\psi|^4 \}, \quad (3)$$

with $q = \partial_x \phi(x)$. The equilibrium supercurrent along the x -direction is

$$I = -2e(2\gamma q + 4\gamma' q^3 + \kappa_1 h + 3\kappa_3 h q^2) |\psi|^2. \quad (4)$$

$|\psi|$ is determined by minimizing F which leads to $|\psi|^2 = \frac{|\alpha|}{\beta} (1 - \frac{\gamma}{|\alpha|} q^2 - \frac{\gamma'}{|\alpha|} q^4 - \sum_{n=1,3} \frac{\kappa_n h}{|\alpha|} q^n)$. Substitution this into Eq. (4) yields

$$I = -2e \frac{|\alpha|}{\beta} \sqrt{|\alpha| \gamma} (1 - \tilde{q}^2 - \tilde{\gamma}' \tilde{q}^4 - \tilde{\kappa}_1 \tilde{q} - \tilde{\kappa}_3 \tilde{q}^3) \times (2\tilde{q} + 4\tilde{\gamma}' \tilde{q}^3 + \tilde{\kappa}_1 + 3\tilde{\kappa}_3 \tilde{q}^2), \quad (5)$$

with the dimensionless variables defined as $\tilde{q} = q \sqrt{\gamma/|\alpha|}$, $\tilde{\gamma}' = \gamma' |\alpha| / \gamma^2$, and $\tilde{\kappa}_n = n \kappa_n h |\alpha|^{n/2-1} \gamma^{-n/2}$.

Since γ, γ' are always positive, Eq. (5) results in a maximum I_{c+} and a minimum $-I_{c-}$, with $I_{c\pm}$ being the critical currents along the positive and negative directions respectively. Assuming $\tilde{\gamma}', \tilde{\kappa}_{1,3} \ll 1$ which is true for small h , one obtains,

$$I_{c\pm} \approx 2e \frac{\sqrt{|\alpha|^3 \gamma}}{\beta} \left\{ \frac{4(1 + \tilde{\gamma}')}{3\sqrt{3}} \pm [\tilde{\kappa}_3(1 + 2\tilde{\gamma}') - 2\tilde{\kappa}_1 \tilde{\gamma}'] \right\}, \quad (6)$$

which are not equal, resulting in the superconductor diode effect. Let us define the following SC diode quality parameter,

$$Q \equiv \frac{I_{c+} - I_{c-}}{\frac{1}{2}(I_{c+} + I_{c-})} = 2[\tilde{\kappa}_3(1 + 2\tilde{\gamma}') - 2\tilde{\kappa}_1 \tilde{\gamma}'] \approx 2\tilde{\kappa}_3. \quad (7)$$

It turns out that either $\gamma' \neq 0$ or $\kappa_3 \neq 0$ is required to achieve SC diode effect. The κ_1 term alone (i.e. $\gamma' = \kappa_3 = 0$) is not enough to do that because it simply shifts the equilibrium value of q by a constant ($-\kappa_1 h / 2\gamma$), like a gauge transformation. That does not affect $I_{c\pm}$ since the current operator contains a term proportional to κ_1 , see Eq. (4), which cancels the shift of the equilibrium q .

For examples of SC diode effects, let us consider the following typical state-of-art two-dimensional systems: (i) Rashba SCs, (ii) surfaces of topological insulator (TI), and (iii) Ising SCs. While the first two have similar spin-momentum lockings, the last one has a very different form.

Rashba system — The Hamiltonian of a 2D system with Rashba spin-orbit coupling can be written as

$$H_R(\mathbf{k}) = \left(\frac{k^2}{2m} - \mu \right) \sigma_0 + \lambda_R (k_x \sigma_y - k_y \sigma_x) + \mathbf{h} \cdot \boldsymbol{\sigma}, \quad (8)$$

	\mathcal{P}_{x1}	\mathcal{P}_{x2}
$h_x \sigma_x$	+	-
$h_y \sigma_y$	-	-
$h_z \sigma_z$	-	+

TABLE I. Symmetry operations on the Zeeman fields along the three directions in Rashba systems. A plus (minus) sign means that the Zeeman term is even (odd) under the symmetry operation.

where λ_R is the Rashba spin-orbit coupling strength, $\mathbf{k} = (k_x, k_y)$ is the electron wave vector, h is the magnetic field, and $\sigma_{x,y}$ are Pauli matrices (the physical constants \hbar, μ_B, k_B all being unity throughout this manuscript). Two x -inverting symmetries, $\mathcal{P}_{x1} = \sigma_x$ and $\mathcal{P}_{x2} = \sigma_z$, are preserved when $\mathbf{h} = \mathbf{0}$. Their effects on magnetic fields along different directions are shown in TABLE I. To break a symmetry, the Zeeman term must be odd under the symmetry operation. TABLE I shows that only a Zeeman field along the y -direction breaks both \mathcal{P}_{x1} and \mathcal{P}_{x2} . According to the previous analysis, nonreciprocity in the $\pm x$ -directions can be expected if $h_y \neq 0$.

The Rashba SOC results in the following term of the GL free energy (to the linear order in h),

$$\delta F_R = \int d\mathbf{q} (q_x h_y - q_y h_x) (\kappa_1^R + \kappa_3^R |\mathbf{q}|^2) |\psi_{\mathbf{q}}|^2. \quad (9)$$

Thus, if a magnetic field along the y -direction, $\mathbf{h} = (0, h_y)$, is applied, the critical currents along the $\pm x$ -direction will be different, as previously obtained in Eq.s (6-7) and consistent with the symmetry analysis. The corresponding SC diode quality parameter as defined in Eq. (7) is (neglecting γ')

$$Q_{\mu > 0}^R = \frac{18\pi h_y}{\lambda_R \sqrt{m E_R}} \sqrt{\frac{T_c(T_c - T)}{14\zeta(3)E_R^2}} \frac{1}{(1 + \mu/E_R)^{5/2}}, \quad (10)$$

$$Q_{\mu < 0}^R = \frac{45\pi h_y}{\lambda_R \sqrt{m E_R}} \sqrt{\frac{T_c(T_c - T)}{14\zeta(3)E_R^2}} \frac{1}{(1 + \mu/E_R)^{7/4}}, \quad (11)$$

where $\zeta(x)$ is the Riemann zeta function and $E_R = m\lambda_R^2/2$. The functional form depends on the sign of μ . For a given λ_R , the strength of the SC diode effect, denoted by Q^R , increases quickly as μ decreases, especially when the band bottom is approached with $\mu \gtrsim -E_R$, as shown in FIG. 1a. Furthermore, a discontinuity appears at $\mu = 0$, which is due to the change of the spin-momentum locking direction (helicity). Note that the GL theory breaks down near the band edge and near $\mu = 0$. Thus the divergence is illusive and the discontinuity will be smoothed out.

TI surface — For a TI surface, the effective Hamiltonian takes the same form as Eq. (8) and share the same symmetries. The free energy δF_T has a similar form as in Eq. (9). However, λ_R should be replaced by v , the

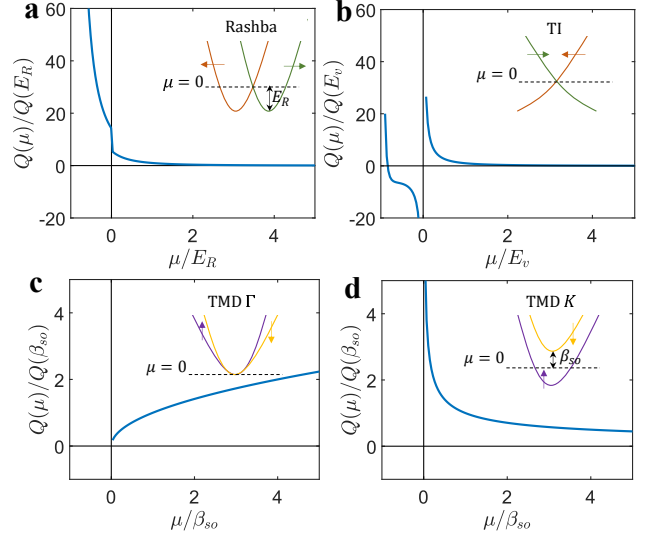


FIG. 1. The superconductor (SC) diode quality parameter Q of various spin-orbit coupled systems as functions of the chemical potential μ . **a.** Rashba superconductors; **b.** Superconducting surface states of topological insulators (TIs); **c.** The Γ -pockets of the Ising SCs in transition metal dichalcogenides (TMDs). **d.** The K -pockets of SC TMDs. The schematic band structures of various systems with spin-orbit coupling are shown in the insets correspondingly. The reference point of $\mu = 0$ is shown for each case.

Fermi velocity at the $k = 0$ point, and both v and m are large. Instead of E_R , the energy scale corresponding to the spin-orbit coupling becomes $E_v = mv^2/2$. Another difference from the Rashba system is that there is only one Fermi surface as shown in the insets of FIG. 1a-b. With all these taken into account, we obtain the quality parameter for this system

$$Q^T = \frac{9\pi h_y T_c}{\sqrt{14\zeta(3)E_v^2}} \sqrt{1 - \frac{T}{T_c}} \frac{\text{Sign}[v\tilde{\mu}](5\sqrt{1+\tilde{\mu}}-2)}{(1+\tilde{\mu})^2|\sqrt{1+\tilde{\mu}}-1|}. \quad (12)$$

We have defined $\tilde{\mu} = \mu/E_v$. As we can see in FIG. 1b, Q^T diverges at both $\mu = 0$ and $\mu = -E_v$. But we should emphasize that no divergence of Q^T is really predicted here at $\mu = 0$ because the GL method (the expansion over q) we adopt is not valid any more when $k_F \gg |q|$ no longer holds ($k_F \approx \mu/v$ is the Fermi wave vector). A special feature of the TI surface is that the sign of Q^T is flipped when μ (not near the band edge at $\mu \approx -E_v$) changes its sign.

Ising SCs — Found in thin films of transition metal dichalcogenides (TMDs) (NbSe₂, MoS₂, etc.), Ising SCs [21–25] have a special kind of spin-orbit coupling where the electron spins are strongly pinned in the z -direction, making the effects of in-plane Zeeman field negligible. We consider an out-of-plane field h_z . There may be two kinds of Fermi pockets in TMDs, near the Γ and the K/K'

points respectively in the Brillouin zone. The effective Hamiltonian of a mono-layer TMD near the Γ point can be written as

$$H_\Gamma = \left(\frac{k^2}{2m} - \mu\right)\sigma_0 + \lambda_I(k_x^3 - 3k_x k_y^2)\sigma_z + h_z\sigma_z. \quad (13)$$

There are two x -inverting symmetries $\mathcal{P}_{x1} = \sigma_x$ and $\mathcal{P}_{x2} = \sigma_y$. As a result, $h_z \neq 0$, which breaks both of them, is required to achieve nonreciprocity in $\pm x$ -directions. On the other hand, $\mathcal{P}_{y,1/2/3} = \sigma_{x/y/z}$ and thus the nonreciprocity in $\pm y$ -directions does not exist.

The Ising SOC results in a term of the free energy,

$$\delta F_\Gamma = h_z \kappa_3^\Gamma \int d\mathbf{q} (q_x^3 - 3q_x q_y^2) |\psi_{\mathbf{q}}|^2, \quad (14)$$

which leads to the SC diode effect with the quality parameter,

$$Q^\Gamma = \frac{1116\zeta(5)}{[7\zeta(3)]^{3/2}} h_z \lambda_I m^{3/2} \sqrt{\frac{\mu}{T_c}} \sqrt{1 - \frac{T}{T_c}}, \quad (15)$$

when the currents flow in the $\pm x$ -directions. Equation (14) indicates that Q^Γ changes its sign as the measurement direction is rotated in the x - y plane (note that $q_x^3 - 3q_x q_y^2 = |\mathbf{q}|^3 \cos 3\theta_{\mathbf{q}}$), manifesting the three-fold rotational symmetry of the TMDs. On the other hand, near the K and K' points of the Brillouin zone, the effective Hamiltonian can be written as $H_{\text{TMD},K} = \frac{k^2}{2m} - \mu + \tau\beta_{so}\sigma_z + h_z\sigma_z$, where $\tau = \pm 1$ for the K and K' pockets respectively, and β_{so} is the Ising spin-orbit splitting energy. The free energy contains no inversion symmetry breaking terms and thus $I_{c\pm}$ are equal. However, if a band warping term $\lambda_{\text{warp}}(q_x^3 - 3q_x q_y^2)$ is added, it also leads to the SC diode effect and

$$Q^K = \frac{1116\zeta(5)}{[7\zeta(3)]^{3/2}} h_z \lambda_{\text{warp}} m^{3/2} \frac{2\beta_{so}}{\mu} \sqrt{\frac{\mu}{T_c}} \sqrt{1 - \frac{T}{T_c}}. \quad (16)$$

The μ -dependences of the Q^Γ and Q^K are shown in FIG. 1c-d. A distinct feature of Q^Γ is that $Q^\Gamma \rightarrow 0$ when μ approaches the band edge, while the others $Q^{R/T/K}$ diverge there. In TMDs with both Γ and K pockets, they should be considered simultaneously in the Free energy. It is not a simple summation of Q^Γ and Q^K . One should also note that μ is defined here relative to different reference points for each of the two parts.

Josephson junctions

Consider an S-N-S junction where two SCs are connected by a normal Rashba metal. The middle normal region acquires a finite superconductivity order parameter $\psi(\mathbf{r})$ due to proximity effect. Assuming that $\psi(\mathbf{r})$ only varies in the x -direction, we obtain from Eq. (3) the following one-dimensional GL equation,

$$[\alpha - \gamma\partial_x^2 + h\kappa_1(-i\partial_x) + h\kappa_3(-i\partial_x)^3]\psi(x) = 0. \quad (17)$$

This corresponds to a generalization of the equation in Reference [12] to include the third order derivative. We have neglected β and γ' assuming both $\psi(x)$ and $\partial_x\psi(x)$ to be small in the junction region. We also assume $\alpha > 0$ so that the middle region alone would be in the normal state and the order parameter is only induced by the proximity effect. Using the ansatz $\psi_q(x) = \psi_0 e^{iqx}$, we obtain the solution by solving for q in Eq. (17), similar to Reference [12]. There are three solutions, $q_\pm = q_0 \pm i/\xi$ and $q' \approx -\gamma/h\kappa_3$, where $q_0 = \frac{h}{2\gamma}(\frac{\alpha\kappa_3}{\gamma} - \kappa_1)$ and $\xi = \sqrt{\gamma/\alpha}$. When h is small, $q' \rightarrow \infty$ corresponds to a very strongly oscillating order parameter. For a long junction under a weak field, the order parameter should be slowly varying and we neglect the q' component. Then the full solution is $\psi(x) = \psi_0(c_+ e^{iq_+x} + c_- e^{iq_-x})$. The coefficients c_\pm are determined by the boundary conditions $\psi(\pm L/2) = \Delta e^{\pm i\phi/2}$, where L is the length of the junction and ϕ is the Josephson phase. Applying the real-space version of Eq. (4) to the solution of $\psi(x)$, we obtain the Josephson current,

$$I^J = 8e|\Delta|^2 \exp[-\frac{L}{\xi}] \sqrt{\alpha\gamma} [\sin(q_0 L - \phi) - \tilde{\kappa}_3]. \quad (18)$$

The difference between the critical currents along $\pm x$ -directions is

$$\delta I_c^J = 8e|\Delta|^2 \sqrt{\alpha\gamma} \exp[-\frac{L}{\xi}] \tilde{\kappa}_3. \quad (19)$$

And the quality parameter is

$$Q^J \equiv 2(I_{c+}^J - I_{c-}^J)/(I_{c+}^J + I_{c-}^J) \approx 2\tilde{\kappa}_3, \quad (20)$$

the same as Eq.(7) except that α is positive here.

The previous calculations are valid for long junctions near the transition temperature under a weak field. In the following, we calculate the Josephson current numerically using a tight-binding model of the Rashba Josephson junction. The supercurrent is given by

$$I^J(\mathbf{h}, \phi) = -\partial_\phi \sum_n f(\varepsilon_n) \varepsilon_n(\mathbf{h}, \phi), \quad (21)$$

where ε_n is the energy eigenvalue of the n -th Andreev bound state and $f(\varepsilon)$ is the Fermi distribution function. Suppose that the junction is homogeneous along the transverse directions, then the summation can be written as $\sum_{n,\mathbf{k}_\perp} f(\varepsilon_n) \varepsilon_{n,\mathbf{k}_\perp}$ with \mathbf{k}_\perp denoting the transverse wave vectors. In centrosymmetric systems, the inversion symmetry \mathcal{P} guarantees $\varepsilon_{n,\mathbf{k}_\perp}(\mathbf{h}, \phi) = \varepsilon_{n,-\mathbf{k}_\perp}(\mathbf{h}, -\phi)$ which, according to Eq. (21), leads to an antisymmetric current phase relation $I^J(\mathbf{h}, \phi) = -I^J(\mathbf{h}, -\phi)$ and thus $I^J(\mathbf{h}, \phi = 0) = 0$. Breaking \mathcal{P} is necessary but, however, not sufficient, to obtain nonreciprocal currents. Suppose that \mathcal{P} is broken while \mathcal{P}_x is preserved (assuming that the current $I^J(\phi)$ flows along x -direction), then the relation between $\varepsilon_{n,\mathbf{k}_\perp}$ and $\varepsilon_{n,-\mathbf{k}_\perp}$ is lost. However, changing back to the notation of Eq. (21) where

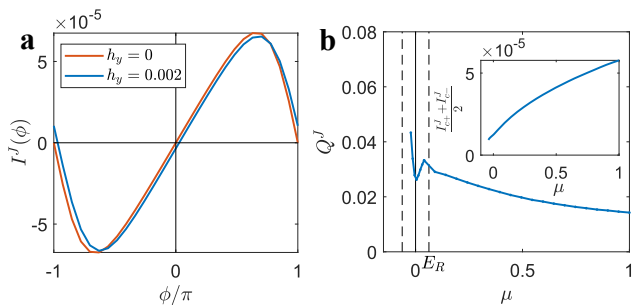


FIG. 2. **a**. The current phase relations for a Josephson junction with Rashba spin-orbit interaction, calculated with Eq.(22) without and with Zeeman fields along the y -direction ($\mu = 0.2$). **b**. The Josephson diode quality parameter $Q^J \equiv 2(I_{c+}^J - I_{c-}^J)/(I_{c+}^J + I_{c-}^J)$ as a function of the chemical potential μ (with $h_y = 0.002$). The inset in **b** shows the direction-independent (averaged) part of the critical current. Other parameters: $m = 0.5$, $\lambda_R = 0.5$, $\mu = 1$, $\Delta = 0.01$, $T = 0.0025$. The size of the S-N-S junction in numbers of sites is 150-5-150.

n includes the transverse wave vectors, it still holds that $\varepsilon_n(\mathbf{h}, \phi) = \varepsilon_n(\mathbf{h}, -\phi)$ due to \mathcal{P}_x and one still gets anti-symmetric CPR. Thus, we arrive in a different way at our previous conclusion — the symmetry \mathcal{P}_x must be broken to obtain nonreciprocity, i.e. asymmetric CPR.

To calculate the Josephson current numerically for generic situation, we write down a lattice Bogoliubov-de Gennes Hamiltonian based on the continuum model in Eq. (8),

$$\begin{aligned}
 H_R = & \sum_{\mathbf{r}} \sum_{s=\uparrow\downarrow} \left\{ \frac{1}{2m} [c_s^\dagger(\mathbf{r})c_s(\mathbf{r} + \hat{x}) + c_s^\dagger(\mathbf{r})c_s(\mathbf{r} + \hat{y})] \right. \\
 & + \frac{\lambda_R}{2} [c_s^\dagger(\mathbf{r})c_{-s}(\mathbf{r} + \hat{x}) - ic_s^\dagger(\mathbf{r})c_{-s}(\mathbf{r} + \hat{y})] \\
 & \left. + \Delta(\mathbf{r})c_s(\mathbf{r})c_{-s}(\mathbf{r}) \right\} + h.c. - \mu c_s^\dagger(\mathbf{r})c_s(\mathbf{r}). \quad (22)
 \end{aligned}$$

The field operator $c_s(\mathbf{r})$ ($c_s^\dagger(\mathbf{r})$) annihilates (creates) an electron with spin $s = \uparrow\downarrow$ on the site \mathbf{r} of a square lattice, where nearest neighbors are connected by the unit vectors \hat{x} and \hat{y} in the x - and y -directions respectively. The pairing amplitude is $\Delta(\mathbf{r}) = \Delta e^{-i\phi/2}$ when $x < -L/2$, $\Delta(\mathbf{r}) = 0$ when $-L/2 < x < L/2$, and $\Delta(\mathbf{r}) = \Delta e^{i\phi/2}$ when $x > L/2$. The current is obtained by diagonalizing Eq. (22) and then applying Eq. (21).

When a field \mathbf{h} along x - or z -direction is applied, the CPR is exactly antisymmetric and $I_{c\pm}$ are equal, consistent with our previous symmetry analysis. The CPRs without magnetic field and with a small field along the y -direction are shown in FIG. 2a. When $h_y \neq 0$, the $\phi = 0$ junction has a finite Josephson current. The new ground state with zero I^J acquires a phase difference (the ϕ_0 -junctions [12–17, 19, 20, 26–34]), as predicted in Eq. (18) and in Reference [12]. Besides the shift of ground state phase difference, the critical currents $I_{c\pm}^J$ become unequal. The diode quality parameter $Q^J \equiv 2(I_{c+}^J - I_{c-}^J)/(I_{c+}^J + I_{c-}^J)$ is shown in FIG. 2b for a

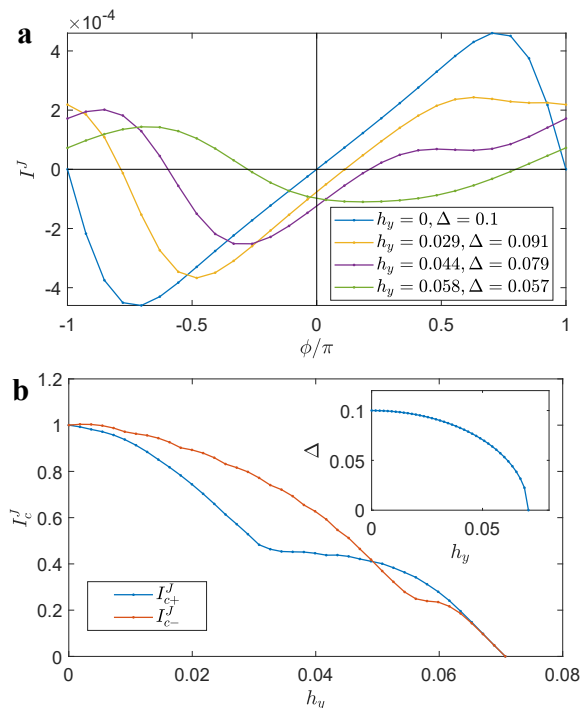


FIG. 3. **a**. The current-phase relations (CPR) with various values of the magnetic field h_y along the y -direction. **b**. The critical currents along $\pm x$ directions as functions of h_y . The inset shows the simplified relation between the superconducting gap Δ and the field h_y .

varying chemical potential μ , which is qualitatively consistent with the GL theory prediction in Eq. (20) and as shown in FIG. 1a. Strong deviation appears near $\mu = 0$ and $\mu = -E_R$ because the GL method breaks down there, as mentioned previously.

The GL theory here does not apply with large field. We show with numerical results that the Josephson diode effect observed in [10] is due to Rashba spin-orbit coupling. A magnetic field h_y is applied with its strength varying from zero to the size of the SC gap. The resulting CPRs are shown in FIG. 3a where the asymmetry is obvious when $h_y \neq 0$. The critical Josephson currents along $\pm x$ -directions are shown in FIG. 3b. Note that we consider the magnetic-field-induced reduction of the SC gap by varying Δ with h_y with the simplified relation $\Delta = 0.1 \times (1 - h_y^2/H_c^2)^{1/2}$ (see the inset of FIG. 3b). The results capture the essential features observed in [10].

DISCUSSION

We have shown that the superconductor diode effect in single superconductors and in Josephson junctions can be understood in a unified picture with the Ginzburg-Landau theory. It originates from the magnetochiral anisotropy induced by various kinds of spin-orbit cou-

pling (SOC). In systems with Rashba SOC, or near the K -points of transition metal dichalcogenides, the weight of the nonreciprocal part of the supercurrent is greatly enhanced when the SOC strength increases or when the chemical potential decreases. On a superconducting surface of topological insulators, the enhancement also happens near the band crossing point, across which the nonreciprocal part flips its sign.

Although we have shown that the ratio between the nonreciprocal part and the reciprocal part of the supercurrent, $Q \equiv I_{c,nr}/I_{c,r}$, can be gigantic near the band edge and, for TI surfaces, near the band crossing point, one should note that it comes with a reduced total supercurrent I_c . This is seen in the inset of FIG. 2b for a Josephson junction. Similar situation happens to the choice of the strength of the magnetic field h . Increasing h enhances Q but reduces I_c at the same time. Thus, the optimal position of the chemical potential shall be determined by a balance between Q and I_c .

When we were finalizing our manuscript, we noticed a recent paper [35] on a related topic and were informed that another group [36] had been working on a similar problem.

MATERIALS AND METHODS

The GL Coefficients

In Rashba SCs, the GL coefficients can be obtained based on Reference [5]. They are

$$\alpha^R = \frac{m(T - T_c)}{\pi T_c} \times \begin{cases} 1 & \text{if } \mu > 0, \\ (1 + \tilde{\mu})^{-1/2} & \text{if } \mu < 0, \end{cases} \quad (23)$$

$$\gamma^R = \frac{7\zeta(3)}{(2\pi T)^2} \frac{E_R}{4\pi} \times \begin{cases} 1 + \tilde{\mu} & \text{if } \mu > 0, \\ (1 + \tilde{\mu})^{1/2} & \text{if } \mu < 0, \end{cases} \quad (24)$$

$$\kappa_3^R = \frac{105\zeta(3)}{128\pi^3 T^2 m \lambda_R} \times \begin{cases} \frac{2}{5}(1 + \tilde{\mu})^{-1} & \text{if } \mu > 0, \\ (1 + \tilde{\mu})^{-1/2} & \text{if } \mu < 0, \end{cases} \quad (25)$$

where $\zeta(x)$ is the Riemann zeta function, $\tilde{\mu} = \mu/E_R$, and $E_R = \frac{1}{2}m\lambda_R^2$.

For the TI surface states,

$$\alpha^T = \frac{m(T - T_c)}{2\pi T_c} \left| 1 - \frac{1}{\sqrt{1 + \tilde{\mu}}} \right|, \quad (26)$$

$$\gamma^T = \frac{7\zeta(3)}{32\pi^3 T_c^2} E_v \left| 1 + \tilde{\mu} - \sqrt{1 + \tilde{\mu}} \right|, \quad (27)$$

$$\kappa_3^T = \frac{21\zeta(3)}{128\pi^3 T_c^2} \frac{1}{mv} \frac{\text{Sign}[\tilde{\mu}]}{1 + \tilde{\mu}} \left(\frac{5}{2} \sqrt{1 + \tilde{\mu}} - 1 \right). \quad (28)$$

with $\tilde{\mu} = \mu/E_v$ and $E_v = mv^2/2$.

For the Γ pockets of transition metal dichalcogenides,

$$\alpha^\Gamma = \alpha^K = \frac{4\pi^2 T_c}{7\zeta(3)\mu} (T - T_c), \quad (29)$$

$$\gamma^\Gamma = \gamma^K = \frac{1}{4m}, \quad (30)$$

$$\kappa_3^\Gamma = \frac{93\zeta(5)\mu\lambda_I}{14\zeta(3)(2\pi T_c)^2}, \quad \kappa_3^K = \frac{93\zeta(5)\beta_{so}\lambda_{\text{warp}}}{7\zeta(3)(2\pi T_c)^2}. \quad (31)$$

With these GL coefficients, the SC diode quality parameters are obtained by substituting them respectively into

$$Q \approx 2\tilde{\kappa}_3 = 6h\kappa_3|\alpha|^{1/2}\gamma^{-3/2}. \quad (32)$$

Derivation of Eq. (18)

Equation (17) leads to, $\alpha + \gamma q^2 + h\kappa_1 q + h\kappa_3 q^3 = 0$. Assuming $h\kappa_3$ to be small, we solve the quadratic equation with $\kappa_3 = 0$ first, i.e. $\alpha + \gamma q^2 + h\kappa_1 q = 0$ and obtain the zeroth-order solutions q_\pm . And then we substitute them into the q^3 term, solve $\alpha + \gamma q^2 + h\kappa_1 q + h\kappa_3 q_\pm^3 = 0$, and obtain four first-order solutions. By requiring that they are close to the zeroth order ones, the two desired solutions are obtained, $q_\pm = q_0 \pm iq_1$. The third solution $q' \approx -\gamma/h\kappa_3$ is obtained by Mathematica with the higher order terms of h dropped. Neglecting the fast oscillating q' -component, the order parameter becomes

$$\psi(x) = \Delta [c_+ e^{iq_0 x - q_1 x} + c_- e^{iq_0 x + q_1 x}] \quad (33)$$

with (in the long junction limit $q_1 L \gg 1$)

$$c_\pm = e^{-q_1 L/2} e^{\pm i(q_0 L/2 - \phi/2)}. \quad (34)$$

The Josephson current is

$$I^J = -2e (2\gamma \text{Im}[\psi^* \partial_x \psi] + h\kappa_1 |\psi|^2 + 3h\kappa_3 |\partial_x \psi|^2)_{x=0}. \quad (35)$$

Substitution of Eq.(33) into this equation yields Eq. (18).

ACKNOWLEDGMENTS

N.N. was supported by Ministry of Education, Culture, Sports, Science, and Technology Nos. JP24224009 and JP26103006, JSPS KAKENHI Grant numbers 18H03676 and 26103006, and Core Research for Evolutionary Science and Technology (CREST) No. JPMJCR16F1 and No. JPMJCR1874, Japan. Y. T. is supported by Scientific Research (A) (KAKENHI Grant No. JP20H00131), Scientific Research (B) (KAKENHI Grants No. JP18H01176 and No. JP20H01857), Japan-RFBR Bilateral Joint Research Projects/Seminars No. 19-52-50026, and the JSPS Core-to-Core program ‘‘Oxide Superspin’’ international network. J.J.H. was supported by RIKEN Incentive Research Projects.

-
- [1] Y. Tokura and N. Nagaosa, *Nat. Commun.* 9, 3740 (2018).
- [2] D. Xiao, M. C. Chang, and Q. Niu, *Rev. Mod. Phys.* 82, 1959 (2010).
- [3] N. Nagaosa and T. Morimoto, *Adv. Mater.* 29, 1603345 (2017).
- [4] R. Wakatsuki, Y. Saito, S. Hoshino, Y. M. Itahashi, T. Ideue, M. Ezawa, Y. Iwasa, and N. Nagaosa, *Sci. Adv.* 3, e1602390 (2017).
- [5] R. Wakatsuki and N. Nagaosa, *Phys. Rev. Lett.* 121, 026601 (2018).
- [6] S. Hoshino, R. Wakatsuki, K. Hamamoto, and N. Nagaosa, *Phys. Rev. B* 98, 054510 (2018).
- [7] K. Yasuda, H. Yasuda, T. Liang, R. Yoshimi, A. Tsukazaki, K. S. Takahashi, N. Nagaosa, M. Kawasaki, and Y. Tokura, *Nat. Commun.* 10, 2734 (2019).
- [8] G. L. J. A. Rikken, J. Fölling, and P. Wyder, *Phys. Rev. Lett.* 87, 236602 (2001).
- [9] F. Ando, Y. Miyasaka, T. Li, J. Ishizuka, T. Arakawa, Y. Shiota, T. Moriyama, Y. Yanase, and T. Ono, *Nature* 584, 373 (2020).
- [10] C. Baumgartner, L. Fuchs, A. Costa, S. Reinhardt, S. Gronin, G. C. Gardner, T. Lindemann, M. J. Manfra, P. E. F. Junior, D. Kochan, J. Fabian, N. Paradiso, and C. Strunk, *ArXiv: 2103.06984* (2021).
- [11] J. Hu, C. Wu, and X. Dai, *Phys. Rev. Lett.* 99, 067004 (2007).
- [12] A. Buzdin, *Phys. Rev. Lett.* 101, 107005 (2008).
- [13] A. A. Reynoso, G. Usaj, C. A. Balseiro, D. Feinberg, and M. Avignon, *Phys. Rev. Lett.* 101, 107001 (2008).
- [14] A. Zazunov, R. Egger, T. Jonckheere, and T. Martin, *Phys. Rev. Lett.* 103, 147004 (2009).
- [15] I. Margaritis, V. Paltoglou, and N. Flytzanis, *J. Phys. Condens. Matter* 22, 445701 (2010).
- [16] T. Yokoyama, M. Eto, and Y. V. Nazarov, *Phys. Rev. B* 89, 195407 (2014).
- [17] F. Dolcini, M. Houzet, and J. S. Meyer, *Phys. Rev. B* 92, 035428 (2015).
- [18] C.-Z. Chen, J. J. He, M. N. Ali, G.-H. Lee, K. C. Fong, and K. T. Law, *Phys. Rev. B* 98, 075430 (2018).
- [19] S. Pal and C. Benjamin, *EPL* 126, 57002 (2019).
- [20] A. A. Kopasov, A. G. Kutlin, and A. S. Mel'nikov, *Phys. Rev. B* 103, 144520 (2021).
- [21] J. M. Lu, O. Zheliuk, I. Leermakers, N. F. Q. Yuan, U. Zeitler, K. T. Law, and J. T. Ye, *Science* 350, 1353 (2015).
- [22] Y. Saito, Y. Nakamura, M. S. Bahramy, Y. Kohama, J. Ye, Y. Kasahara, Y. Nakagawa, M. Onga, M. Tokunaga, T. Nojima, Y. Yanase, and Y. Iwasa, *Nat. Phys.* 12, 144 (2016).
- [23] X. Xi, Z. Wang, W. Zhao, J. H. Park, K. T. Law, H. Berger, L. Forró, J. Shan, and K. F. Mak, *Nat. Phys.* 12, 139 (2016).
- [24] N. F. Q. Yuan, B. T. Zhou, W.-Y. He, and K. T. Law, *ArXiv1605.01847* (2016).
- [25] G.-B. Liu, W.-Y. Shan, Y. Yao, W. Yao, and D. Xiao, *Phys. Rev. B* 88, 085433 (2013).
- [26] L. Dell'Anna, A. Zazunov, R. Egger, and T. Martin, *Phys. Rev. B* 75, 085305 (2007).
- [27] Y. Tanaka, T. Yokoyama, and N. Nagaosa, *Phys. Rev. Lett.* 103, 107002 (2009).
- [28] J. -F. Liu and K. S. Chan, *Phys. Rev. B* 82, 184533 (2010).
- [29] M. Alidoust and J. Linder, *Phys. Rev. B* 87, 060503 (2013).
- [30] A. Brunetti, A. Zazunov, A. Kundu, and R. Egger, *Phys. Rev. B* 88, 144515 (2013).
- [31] B. Lu, K. Yada, A. A. Golubov, and Y. Tanaka, *Phys. Rev. B* 92, 100503 (2015).
- [32] F. S. Bergeret and I. V. Tokatly, *EPL (Europhysics Lett.)* 110, 57005 (2015).
- [33] G. Campagnano, P. Lucignano, D. Giuliano, and A. Tagliacozzo, *J. Phys. Condens. Matter* 27, 205301 (2015).
- [34] D. B. Szombati, S. Nadj-Perge, D. Car, S. R. Plissard, E. P. A. M. Bakkers, and L. P. Kouwenhoven, *Nat. Phys.* 12, 568 (2016).
- [35] N. F. Q. Yuan and L. Fu, *arXiv:2106.01909* (2021).
- [36] A. Daido and Y. Yanase, to be published.